Mathematical Geology, Vol. 27, No. 1, 1995

The Perimeter–Area Fractal Model and Its Application to Geology[1]

Qiuming Cheng[2]

Perimeters and areas of similarly shaped fractal geometries in two-dimensional space are related to one another by power-law relationships. The exponents obtained from these power laws are associated with, but do not necessarily provide, unbiased estimates of the fractal dimensions of the perimeters and areas. The exponent (D_{AL}) obtained from perimeter-area analysis can be used only as a reliable estimate of the dimension of the perimeter (D_L) if the dimension of the measured area is $D_A = 2$. If $D_A < 2$, then the exponent $D_{AL} = 2D_L/D_A > D_L$. Similar relations hold true for area and volumes of three-dimensional fractal geometries. The newly derived results are used for characterizing Au associated alteration zones in porphyry systems in the Mitchell-Sulphurets mineral district, northwestern British Columbia.

KEY WORDS: similarly shaped geometries, fractal dimension, area, perimeter, volume, power-law relation.

INTRODUCTION

For a group of similarly shaped sets in two-dimensional space, the ratio of the perimeter (L) and area (A) has the form $\rho = L/\sqrt{A}$. For example, if the sets consist of circles, squares, or equilateral triangles, the values of ρ equal $2\sqrt{\pi}$, 4, and $6/3^{1/4}$, respectively. As a generalization, the following relationship between perimeters and areas for similarly shaped fractal sets was introduced originally by Mandelbrot (1983).

$$L(\delta) = C\delta^{(1-D)}A(\delta)^{D/2} \tag{1}$$

where C is a constant and D was used as the fractal dimension of the perimeter L. This relation depends on the value of the yardstick δ which is used for measurement. Equation (1) has been used extensively in physics, earth sciences, and other fields; for example, for cloud and rain perimeter fractal dimension by

[1]Received 14 January 1994; accepted 26 September 1994.

[2]Ottawa-Carleton Geoscience Centre, University of Ottawa, Ottawa, Ontario K1N 6N5, Canada; e-mail: Cheng@gsc.emr.ca.

0882-8121/95/0100-0069$07.50/1

Lovejoy (1982) and Hentschel and Procaccia (1983); streams and drainage areas (Hack, 1957; Mandelbrot, 1982); fractal dimension of hail clouds (Rys and Waldvogel, 1986); fracture surfaces of titanium specimens (Pande, Richards, and Smith, 1987); perimeters and areas of geochemical landscapes (Bölviken and others, 1992). In these applications, the exponent D in Equation (1) was used for estimating fractal dimension of perimeter or fractal dimension of fractional Brownian surface (D_s) by the relation $D_s = D + 1$ (Mandelbrot, 1983, 1985; Voss, 1985). The technique of slit-island analysis (Mandelbrot, Passoja, and Paullay, 1984) also was based on Equation (1).

The following modified expression was derived by Lovejoy and Schertzer (1991) on the basis of multifractal theory:

$$L(\delta)C\delta^{(1-\xi_T)}A(\delta)^{\xi_T/2} \tag{2}$$

where $\xi_T = 2D(p_T)/D(s_{T\geq})$; $D(p_T)$ and $D(s_{T\geq}) \leq 2$ are fractal dimensions for the perimeter and the area of subsets with concentration values above threshold T. This relation holds for a yardstick δ which is small enough to measure the smallest area accurately. For each value of δ, $L(\delta)$ and $A(\delta)$ satisfy the power-law relation:

$$L(\delta) = C_0 A(\delta)^{\xi_T/2} \tag{3}$$

Korvin (1992) discussed the relationships between length (L), width (W), and area (A) of river and drainage systems and described Hack's (1957) law by the following equations:

$$L \propto W^{P_L}; \quad A \propto W^{P_X + P_Y}; \quad L \propto A^{P_L/(P_X + P_Y)} \tag{4}$$

where $\propto$ denotes proportionality, and P_L, P_X, and P_Y represent the exponents of the power-law relations between L, A, and W, respectively.

Equations (3) and (4) show that length, width, perimeter, and area of river and drainage systems may follow power-law relations. In general, relations between any two different measures for fractal geometries with similar shapes follow power laws. It will be shown that the exponent of a power-law relation of this type is not necessary equal to the fractal dimensions of the two measures although it is associated with them. In this paper, relationships between perimeters, areas, and volumes of similarly shaped geometries will be discussed and the newly derived results illustrated by application to perimeter-area relations for relatively simple examples and also for characterizing Au associated alteration zones in porphyry systems in the Mitchell-Sulphurets mineral district, northwestern British Columbia.

PERIMETER-AREA MODEL

A group of similarly shaped fractal geometries (e.g., islands, landscapes, or three-dimensional objects) can be characterized by their measures for perimeter L, area A, or volume V. The fractal dimensions of perimeter, area, and volume will be denoted as D_L, D_A, and D_V, respectively. When the box-counting method with yardstick δ is used, the estimate length, area, and volume of a geometry can be expressed as:

$$L(\delta) \propto \delta^{(1-D_L)}; \quad A(\delta) \propto \delta^{(2-D_A)}; \quad V(\delta) \propto \delta^{(3-D_V)} \tag{5}$$

and the Hausdorff-Besicovich dimensions D_L, D_A, and D_V can be estimated by following relations:

$$D_L = 1 - \lim_{\delta \to 0} \frac{\log L(\delta)}{\log \delta}; \quad D_A = 2 - \lim_{\delta \to 0} \frac{\log A(\delta)}{\log \delta}; \quad D_V = 3 - \lim_{\delta \to 0} \frac{\log V(\delta)}{\log \delta} \tag{6}$$

For convenience, we take two-dimensional geometries as examples for discussion. Similar relations are valid for three-dimensional objects.

Suppose two sets or objects have similar shapes but different sizes as shown in the example of Figure 1. Size is measured by counting boxes for presence of a feature. The boxes (with widths a and b for the two objects (A and B) which are not of the same size in Figure 1 can be subdivided into smaller boxes with the same size (δ). The numbers of boxes containing perimeter (N_L) (boxes containing both black and blank areas) and area (N_A) of these two objects are proportional to the size of the subareas (δ) according to the relations:

$$N_{L_1} \propto \left(\frac{\delta}{a}\right)^{-D_L}; \quad N_{A_1} \propto \left(\frac{\delta}{a}\right)^{-D_A}$$
$$N_{L_2} \propto \left(\frac{\delta}{b}\right)^{-D_L}; \quad N_{A_2} \propto \left(\frac{\delta}{b}\right)^{-D_A} \tag{7}$$

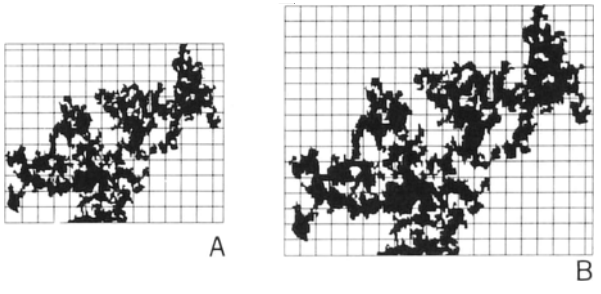

Figure 1. Two similar sets measured with same yardstick.

where D_L and D_A represent the dimensions of the perimeter and area. Therefore, the estimated lengths of perimeters and areas of the two objects can be written as:

$$L_1 \propto \left(\frac{\delta}{a}\right)^{-D_L}\delta; \quad A_1 \propto \left(\frac{\delta}{a}\right)^{-D_A}\delta^2$$
$$L_2 \propto \left(\frac{\delta}{b}\right)^{-D_L}\delta; \quad A_2 \propto \left(\frac{\delta}{b}\right)^{-D_A}\delta^2 \tag{8}$$

From Equation (8), it follows that;

$$\frac{L_1}{L_2} \propto \left(\frac{b}{a}\right)^{-D_L}; \quad \frac{A_1}{A_2} \propto \left(\frac{b}{a}\right)^{-D_A}$$

Therefore,

$$\frac{L_1}{L_2} \propto \left(\frac{A_1}{A_2}\right)^{1/2D_{AL}} \tag{9}$$

where the ratio of perimeters (L_1/L_2) and the ratio of areas (A_1/A_2) satisfy a power-law relation with exponent $D_{AL} = 2D_L/D_A$. This power-law relation is independent of yardstick δ. From Equation (8), we also obtain:

$$L(\delta) = C\delta^{(1-D_{AL})}A(\delta)^{D_{AL}/2} \tag{10}$$

This equation is the same as Equation (2) with $\xi_T = D_{AL}$. It follows that the power-law relationship between $L(\delta)$ and $A(\delta)$ depends on the value of δ.

Similarly, the relations between length and volume and between area and volume can be expressed as:

$$\frac{L_1}{L_2} \propto \left(\frac{V_1}{V_2}\right)^{1/3D_{VL}}; \quad L(\delta) = C\delta^{1-D_{VL}}V(\delta)^{D_{AL}/2}$$
$$\frac{A_1}{A_2} \propto \left(\frac{V_1}{V_2}\right)^{2/3D_{VA}}; \quad A(\delta) = C\delta^{1-D_{VA}}V(\delta)^{2/3D_{VA}} \tag{11}$$

where $D_{VL} = 3D_L/D_V$ and $D_{VA} = 3, D_A/2D_V$. For ordinary geometries with $D_V = 3$, $D_A = 2$, and $D_L = 1$, we have $D_{VA} = D_{VL} = D_{AL} = 1$; and for fractal geometries, D_{VA}, D_{VL}, and $D_{AL} > 1$. If $D_A = 2$ in Equations (9) and (10) corresponds to a two-dimensional set, then $D_{AL} = D_L$. Only in this situation can D_{AL} be used as a reliable estimate of the fractal dimension of the perimeter L. This special situation has been used widely in applications. However, a difference between D_{AL} and D_L has been determined in some applications of perimeter-area analysis. For example, by slit-island analysis, Pande, Richards,

and Smith (1987) obtained dimensions greater than those estimated from resolution-length analysis of vertical sections through the fracture surface used in their study. Goodchild (1988) generated random fractal surfaces by a stochastic process known as fractional Brownian motion, flooding them by water to obtain lakes. He checked the relationships between perimeters and areas of these lakes and concluded that the exponent D_{AL} estimated from his data was significantly less than the theoretical value $D_S - 1$ where D_S is the fractal dimension of the surface. Indeed, if $D_A < 2$, corresponding to fractal sets as will be shown in examples that follow, the exponent D_{AL} is not an unbiased estimate of D_L. Using D_{AL} rather than D_L we are in error by the ratio $2/D_{AL} > 1$ (also see Lovejoy and Schertzer, 1991; Korvin, 1992). The following examples will be used to demonstrate that Equations (9) and (1) are identical only for the situation of $D_A = 2$, but different for $D_A < 2$.

PERIMETER-AREA ANALYSIS FOR FRACTAL SETS

Example 1. Figure 2 shows the construction of a rectangular Euclidian Sierpinski gasket of which the initiator is a rectangle with unit side. The generator eliminates an upper left subrectangle as shown. The striped areas in Figure 2 show the 4th and the 5th generations of this prefractal (cf. Feder, 1988, p. 17).

For the nth generation, the yardstick satisfies $\delta_n = (1/2)^n$, and the estimated length of the perimeter, which includes all edges enclosing the striped area, is

$$L(\delta_n) = 6L(\delta_{n-1}) - 4\delta_n \tag{12}$$

$$L(\delta_n) = 4\left[3^n - \sum_{k=0}^{n-1}(3^{n-1-k})\right]\delta_n = 3^n\left[4 - \frac{4}{3}\sum_{k=0}^{n-1}\left(\frac{1}{3}\right)^k\right]\delta_n$$

$$= 3^n\left[4 - \frac{4}{3}\frac{1}{1-\frac{1}{3}} + o(n)\right]\delta_n = 3^n\,[2 + o(n)]\,\delta_n \tag{13}$$

where $\lim_{n\to\infty} o(n) = 0$. Using the definition of Equations (5) and (6) we obtain:

$$D_L = 1 - \lim_{n\to\infty}\frac{\log\{3^n[2 + o(n)]\delta_n\}}{\log \delta_n} = \frac{\log(3)}{\log(2)} = 1.58$$

The corresponding estimated area is

$$A(\delta_n) = 3^n\delta_n^2 \tag{14}$$

and the fractal dimension D_A can be estimated by definition (5) and (6) as:

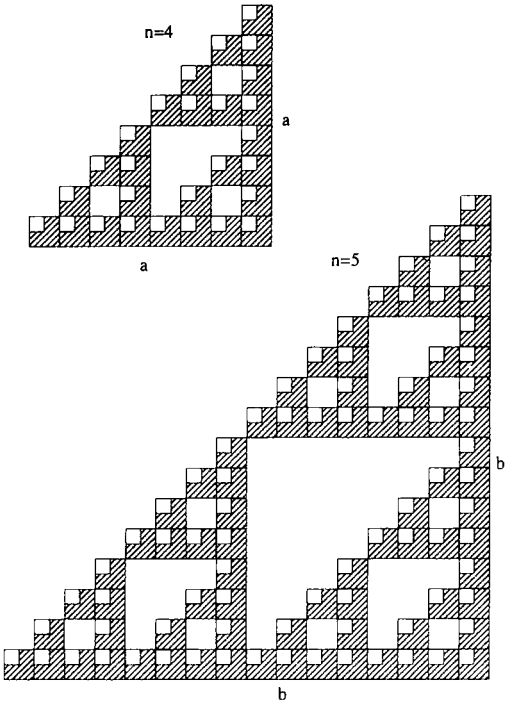

Figure 2. Example 1. Construction of rectangular Euclidian Sierpinski gasket. Initiator is rectangle; generator eliminates upper-left subrectangle with half length of side. Result shown is for 5th generation with $n = 5$ for yardstick $\delta_n = (1/2)^n$. Dimensions of perimeter and area are equal with $D_I = D_A = 1.58$, whereas exponent obtained from perimeter-area relation is $D_{AI} = 2$.

$$D_A = 2 - \lim_{n \to \infty} \frac{\log (3^n \delta_n^2)}{\log \delta_n} = \frac{\log (3)}{\log (2)} = 1.58$$

Therefore, the fractal dimensions are estimated to be: $D_L = D_A = 1.58$. From Equation (9), it then follows that $D_{AL} = 2$. For this example, $D_{AL} \neq D_L$, and Equation (1) is not satisfied.

To verify the relationship between length of perimeter and area, the two generations of the prefractal in Figure 2 can be regarded as objects constructed by using squares with different unit sizes a and b ($a \neq b$) as initiators. Using yardstick δ to measure both length and area, the lengths of perimeters and areas of these two objects are estimated as:

$$L_1(\delta) = \left(\frac{a}{\delta}\right)^{D_L}\delta; \quad A_1(\delta) = \left(\frac{a}{\delta}\right)^{D_A}\delta^2; \quad L_2(\delta) = \left(\frac{b}{\delta}\right)^{D_L}\delta; \quad A_2(\delta) = \left(\frac{b}{\delta}\right)^{D_A}\delta^2$$

Therefore,

$$\frac{L_1(\delta)}{L_2(\delta)} \propto \frac{A_1(\delta)}{A_2(\delta)}; \quad L(\delta) \propto \delta^{-1}A(\delta) \tag{15}$$

These expressions are identical to Equations (8) and (9) with $D_{AL} = 2$.

Example 2. Figure 3 illustrates the construction of a Koch curve with as initiator an equilateral triangle with unit length of sides. Each next generation Koch curve is a curve with sides consisting of four line segments that are 1/3 times as long as those of the previous generation. The 3rd hand 4th generations of this prefractal are shown in Figure 3.

The perimeter and enclosed area of the nth generation prefractal can be estimated from the relations:

$$L(\delta_n) = 3(4)^n\delta_n \tag{16}$$

$$N_A(\delta_n) = N_A(\delta_{n-1})9 + N_L(\delta_{n-1}) \tag{17}$$

where N_A is the number of areas and $N_L(N_L(\delta_n) = 3 \times 4^n)$ is the number of segments, both of which are measured by using the yardstick δ. The length of each yardstick δ_n for the nth generation is

$$\delta_n = (\tfrac{1}{3})^n$$

From Equation (16) it follows that

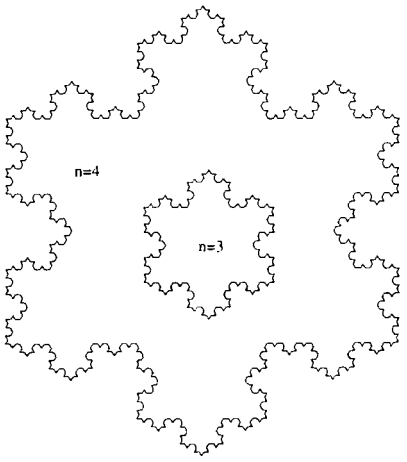

Figure 3. Example 2. Construction of Koch curve. Initiator is triangle. Each segment of initiator is replaced by generator. First generation of this prefractal is curve consisting of four line segments each of length equal to (1/3) of each of laterals. Results shown are for 3rd and 4th generation with $n = 3$ and $n = 4$ for yardstick $(1/3)^n$. For dimensions: $D_L = 1.2618$ and $D_A = 2$; therefore, $D_{AL} = D_L$.

$$D_L = 1 - \lim_{n \to \infty} \frac{\log [3(4)^n \delta_n]}{\log \delta_n} = \frac{\log (4)}{\log (3)} = 1.2618$$

From Equation (17) we have

$$A(\delta_n) = \left| N_A(\delta_0)9^n + \sum_{k=0}^{n-1} N_L(\delta_k)9^{n-1-k} \right| \delta_n^2 = 9^n \left| 1 + \tfrac{1}{3} \sum_{k=0}^{n-1} (\tfrac{4}{9})^k \right| \delta_n^2$$

$$= 9^n [1 + \tfrac{1}{3} \times \tfrac{9}{5} + o(n)] \delta_n^2 = [\tfrac{8}{5} + o(n)] 9^n \delta_n^2 \tag{18}$$

Consequently, the dimension of area is

$$D_A = 2 - \lim_{n \to \infty} \frac{\log \{[\frac{8}{5} + o(n)] 9^n \delta_n^2\}}{\log \delta_n} = \frac{\log (9)}{\log (3)} = 2$$

so that $D_{AL} = D_L = 1.2618$. For this example,

$$\frac{L_1(\delta_n)}{L_2(\delta_n)} \propto \left| \frac{A_1(\delta_n)}{A_2(\delta_n)} \right|^{0.6308} \tag{19}$$

and both Equations (1) and (9) are satisfied.

Example 3. Figure 4 shows the constsruction of a set of an initiator that is a triangle. First, nine subtriangles with one-third-length sides are formed. The generator eliminates the triangles except the two in the lower-left and lower-right corners. The first generation consists of two lower triangles. Each new generation is obtained by applying the generator to all remaining triangles. This prefractal results in a geometry with zero perimeter and zero area. The length of yardstick of the nth generation is

$$\delta_n = (\tfrac{1}{3})^n$$

The length and area of the nth generation prefractal are given by

$$L(\delta_n) = 3(2)^n \delta_n \tag{20}$$

$$A(\delta_n) = A_0 2^n \delta_n^2 \tag{21}$$

where $A_0 = 3^{1/2}/4$. It can be estimated that the dimensions of the perimeter and the area are same and $D_L = D_A = 0.6309$, the set is actually the triadic Cantor set. From Equation (8), it follows that $D_{AL} = 2$. Consequently, $D_{AL} \neq D_L$.

Example 4. Figure 5 shows the construction of a set of an initiator that is a triangle. First, 16 subtriangles with one-fourth-length sides are formed. The generator eliminates the triangles except the shaded four. The first generation consists of four triangles linked to the one at the center. Each new generation is obtained by applying the generator to all remaining triangles. This prefractal

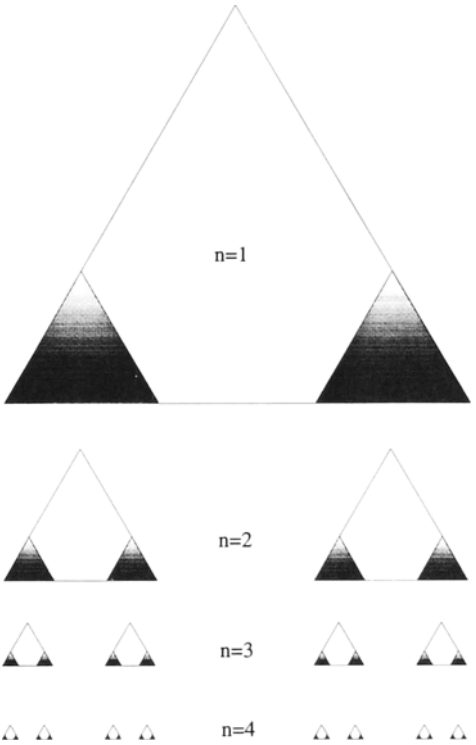

Figure 4. Example 3. Construction of set with fractal dimension $D_L = D_A = 0.6309$. Initiator is triangle. In each generation, triangles are divided into 16 same-shaped triangles; generator eliminates 14 and leaves two small triangles in lower corners. Four generations of prefractal sets are shown in figure. Consequently, D_M (= 2) which is more than three times D_L.

results in a geometry consisting of separate dots. The length of yardstick of the nth generation is

$$\delta_n = (\tfrac{1}{4})^n$$

The length and area of the nth generation prefractal are given by

$$L(\delta_n) = 3(4)^n\delta_n \tag{22}$$

$$A(\delta_n) = A_0 4^n \delta_n^2 \tag{23}$$

where $A_0 = 3^{1/2}/4$. It can be estimated that the dimensions of the perimeter and

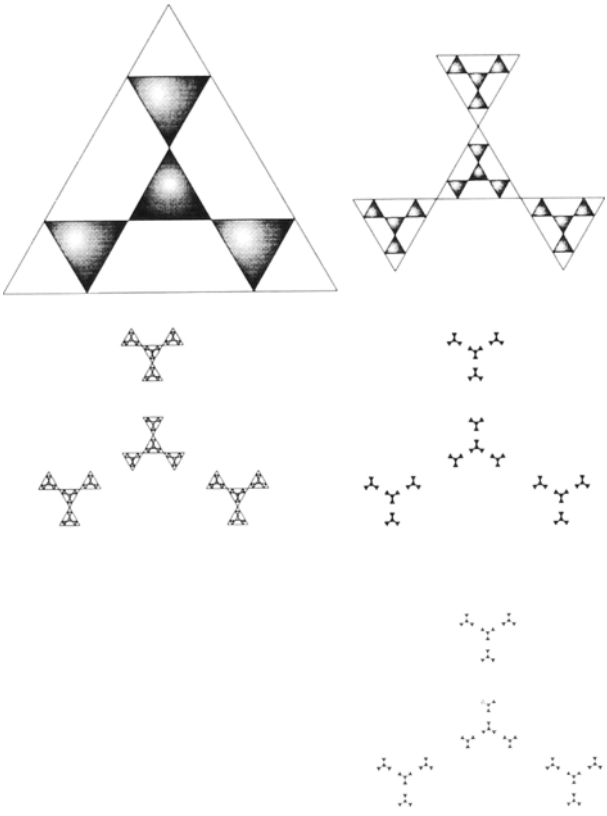

Figure 5. Example 4. Construction of set with fractal dimension $D_L = D_A = 1$. Initiator is triangle. In each generation, triangles are divided into 16 same-shaped triangles; generator eliminates 12 and leaves four triangles connected with one at center. Five generations of prefractal sets are shown.

the area are the same and $D_L = D_A = 1$. From Equation (9), $D_{AL} = 2$, hence $D_{AL} \neq D_L$.

Example 5. Figure 6 shows the construction of a set of an initiator that is a triangle. First, 36 subtriangles with one-sixth-length sides are formed. The generator eliminates those 27 triangles so that the remaining nine triangles are not connected each other. The first generation consists of nine disconnected triangles. Each new generation is obtained by applying the generator to all remaining triangles. The second and third generations are shown in Figure 6. The length of yardstick of the nth generation is

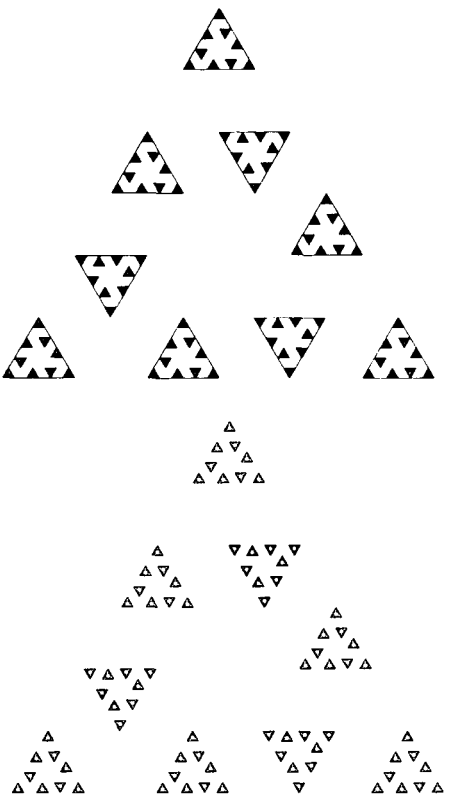

Figure 6. Example 5. Construction of set with fractal dimension $D_L = D_A = 1.2226$. Initiator is triangle. In each generation, triangles are divided into 36 same-shaped triangles; generator eliminates 25 and leaves nine triangles disconnected each other. Second and third generations of prefractal sets are shown.

$$\delta_n = (\tfrac{1}{6})^n$$

The length and area of the nth generation prefractal are given by

$$L(\delta_n) = 3(9)^n\delta_n \tag{24}$$

$$A(\delta_n) = A_0 9^n \delta_n^2 \tag{25}$$

where $A_0 = 3^{1/2}/4$. It can be estimated that the dimensions of the perimeter and the area are the same, and $D_L = D_A = 1.2263$, $D_{AL} = 2$ and $D_{AL} \neq D_L$.

The preceding examples show that the exponent (D_{AL}) from the perimeter-area analysis is not necessarily the same as those of the perimeter and the area. Only if $D_A = 2$ (example 2), $D_{AL} = D_L$ and in this situation the exponent D_{AL} can be used as an unbiased estimate of the fractal dimension of the perimeter. Generally, for $D_A < 2$ (Examples 1, 3, 4, 5), the estimated exponent (D_{AL}) is greater than the fractal dimension of the perimeter ($D_{AL} > D_L$). The examples

3, 4, and 5 show that different sets with dimension D, $0 \leq D \leq 2$ can be constructed from a triangle set by a generator which eliminates a portion of the remaining subtriangles in each generation. For example, the initial triangle can be divided into n^2 small same shaped triangles; in each generation, the generator eliminates $n^2 - n^D$ small triangle and the remaining n^D triangles comprise the prefractal set. The fractal set constructed in this way has fractal dimension of D. Examples 3, 4, and 5 also show that these fractal sets consist of separate points with dimensions $D = 0.6309$, $D = 1$, and $D = 1.2263$, respectively. Therefore, the fractal set (example 4) also can have integer dimension.

PERIMETER-AREA ANALYSIS FOR AU ASSOCIATED GEOCHEMICAL ANOMALIES

Geochemical data (primarily Au) for rock samples collected from an area of 120 km^2 in the Mitchell-Sulphurets district, northwestern British Columbia, can be used to illustrate perimeter-area analysis. This district is considered to have high potential for Au, Au–Ag, and porphyry Cu–Mo mineral resources. Concentration values for Au, Cu, Ag, and As as well as other elements and oxides were used for delineating anomalous areas in Au mineral exploration (Cheng, Agterberg, and Ballantyne, 1994). Figure 7A shows the contour map with geochemical isopleths used for Au, and Figure 7B is the log–log plot

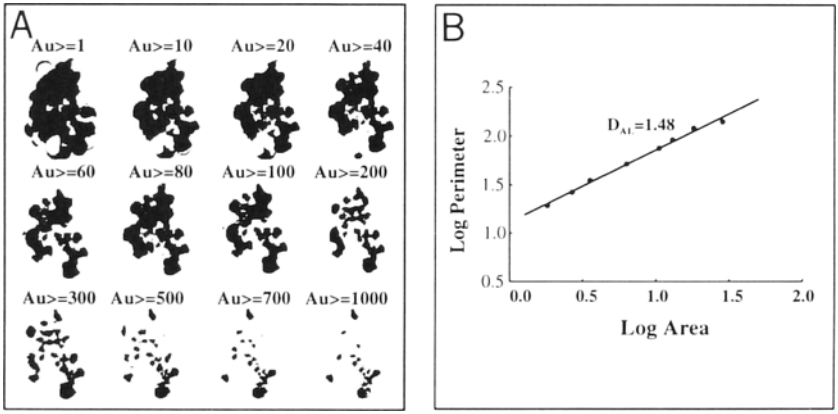

Figure 7. Geochemical anomaly in Mitchell-Sulphurets mineral district, northwestern British Columbia. A, Successive binary patterns for separate contours of Au concentration values from 1033 rock samples. Contours were created by SPANS-GIS potential mapping technique; B, Log-log. plot shows perimeter-area relation for successive contours in Figure 7A. Dots represent values of perimeters and areas of contours with values greater than threshold of 200 ppb and some of these contours are not displayed in Figure 7A. Exponent is estimated to be $D_{A1} = 1.48$.

showing the relationship between perimeters and enclosed areas [Eq. (10)] for separate contours with concentration values greater than the threshold value (Au = 200 ppb) derived for delineating the anomalous areas. The exponent estimated from Figure 7B is $D_{AL} = 1.48$. The outlines of the anomalous areas gave $D_L = 1.24$ (Cheng, Agterberg, and Ballantyne, 1994, fig. 8). From $D_{A1} = 2D_L/D_A$ it followed that $D_A = 1.68$ which is less than 2. It also was estimated that $D_A \approx 2$ for the dimensions of both Cu and As. These results indicate that the distribution of Au in the Mitchell-Sulphurets area is more irregular than that of Cu or As.

CONCLUSIONS

A new model for the relationships between perimeters, areas and volumes of similarly shaped fractal geometries is proposed. It has been shown theoretically and by examples that the fractal dimension estimated from the perimeter-area relation is not necessarily the same as the fractal dimensions of the perimeter and the area. Only if $D_A = 2$, can the exponent (D_{AL}) estimated from the perimeter-area relation be used as unbiased estimate of the fractal dimension of the perimeter. For $D_A < 2$, this exponent is greater than the fractal dimension of the perimeter by the factor $2/D_A > 1$. The perimeter-area model discussed in this paper was used for characterizing anomalous areas of Au, Cu, and As in the Mitchell-Sulphurets area, northwestern British Columbia (Cheng, Agterberg, and Ballantyne, 1994). Gold is more irregularly distributed than Cu and As in this area and the estimated fractal dimensions D_A of anomalous areas for Au, Cu, and As were 1.68, 2, and 2, respectively.

ACKNOWLEDGMENTS

Thanks are due to F. P. Agterberg, Geological Survey of Canada, Ottawa, for careful review, helpful comments, and improvement of English, to S. Dutch, Natural & Applied Sciences, University of Wisconsin-Green Bay, and J. R. Carr, Department of Geological Sciences, University of Nevada, for critical review of the paper and many comments.

REFERENCES

Bölviken, B., Stokke, P. R., Feder, J., and Jössang, T., 1992, The fractal nature of geochemical landscapes: Geochem. Explor., v. 43, no. 2, p. 91-109.

Cheng, Q., Agterberg, F. P., and Ballantyne, B. S., 1994, The separation of geochemical anomalies from background by fractal methods: Geochem. Expl., v. 51, no. 2, p. 109-130.

Feder, J., 1988, Fractals: Plenum Press, New York, 283 p.

Goodchild, M. F., 1988, Lakes on fractal surfaces: A null hypothesis for lake-rich landscapes: Math. Geology, v. 20, no. 6, p. 615-630.

Hack, J. T., 1957, Studies of longitudinal stream profiles in Virginia and Maryland, U.S. Geol. Survey, Prof. Paper 294-B, p. 45–97.

Hentschel, H. G. E., and Procaccia, I., 1983, The infinite number of generalized dimensions of fractals and strange attractors: Physica Ser. D, v. 8, p. 435–444.

Korvin, G., 1992, Fractal models in the earth sciences: Elsevier, Amsterdam, 408 p.

Lovejoy, S., 1982, Area-perimeter relation for rain and cloud areas: Science, v. 216, no. 4542, p. 185–187.

Lovejoy, S., and Schertzer, D., 1991, Multifractal analysis techniques and the rain and cloud fields from 10^{-3} to 10^{6} m, *in* Schertzer, D., and Lovejoy, S., eds., Non-linear variability in geophysics: Kluwer Academic Publ., Dordrecht, p. 111–144.

Mandelbrot, B. B., 1982, The fractal geometry of nature: Freeman, New York, 468 p.

Mandelbrot, B. B., 1983, The fractal geometry of nature (updated and augmented edition): Freeman, New York, 468 p.

Mandelbrot, B. B., 1985, Self-affine fractals and fractal dimension: Physica Scripta, v. 32, no. 4, p. 257–260.

Mandelbrot, B. B., Passoja, D. E., and Paullay, A. J., 1984, Fractal charactistics of fracture surface: Nature, v. 308, no. 5961, p. 721–722.

Pande, C. S., Richards, L. R., and Smith, S., 1987, Fractal characteristics of fractured surface: Jour. Materials Sci. Lett., v. 6, no. 3, p. 295–297.

Rys, F. S., and Waldvogel, A., 1986, Fractal shape of hail clouds: Phys. Rev. Lett., v. 56, no. 7, p. 784–787.

Voss, R. F., 1985, Random fractals: Characterization and measurement, *in* Pynn, R., and Skjeltorp, A., eds., Scaling phenomena in disordered systems: Plenum Press, New York, p. 1–11.